Quantitative Identification of Different Single Molecules by Selective Time-Resolved Confocal Fluorescence Spectroscopy

Joachim R. Fries, Leif Brand, Christian Eggeling, Malte Köllner,† and Claus A. M. Seidel*

Max-Planck-Institut für Biophysikalische Chemie, Am Fassberg 11, D-37077 Göttingen, Germany

Received: January 30, 1998; In Final Form: May 19, 1998

Using a confocal epi-illuminated microscope together with a pulsed laser, new applications of the recently developed, real-time spectroscopic technique BIFL (burst integrated fluorescence lifetime) are introduced. BIFL registers two different types of information on every detected photon with regard to the macroscopic time scale of a measurement and to the fluorescence lifetime. Thus, it is shown to be well suited to identify freely diffusing single dye molecules via their characteristic fluorescence lifetime. This allows for selective counting of dye molecules in an open volume element and opens up the possibility to quantify the relative concentration of the dye molecules, using a recently derived theoretical model, which analyzes the obtained burst size distribution of a sample survey. A closed theory is presented to calculate the probability of a specific dye to cause a fluorescence burst containing a certain number of detected photons. It considers the distribution of the excitation irradiance over the detection volume together with saturation effects of the fluorescence and of the detection electronics, the probability of different transit times through the detection volume, and the probability of multimolecule events. Using BIFL together with selective counting, the concentration of two dyes, Rhodamine B and Rhodamine 6G, in separate solutions and in a mixture were determined. The obtained results are consistent with the applied dye concentrations and with simultaneous measurements by fluorescence correlation spectroscopy (FCS). The introduced method is an appropriate tool for the complete characterization and quantitative analysis of a highly diluted sample in homogeneous assays.

1. Introduction

Laser-induced fluorescence detection is increasingly used as a technique for various ultrasensitive analytical applications in chemistry, biology, and medicine by probing reagents which are either autofluorescing or tagged with a fluorescent dye molecule. The ability to detect and even to identify a single fluorescent molecule via its characteristic fluorescence properties [1−5] opens up a wide range of new opportunities such as sorting and counting single molecules,[6] rare event detection, probe-target binding, and single-molecule DNA sequencing,[7,8] as well as monitoring of single-molecule dynamics.[9]

Different experimental approaches are used to achieve single-molecule detection (SMD) in solution. However, the ability to detect a single molecule is not as much an issue of sensitive detection as a question of background reduction. Thus, the nonspecific background generated by Raleigh and Raman scattering of the solvent and by fluorescent impurities in the solvent[10] must be discriminated by tight spectral and spatial filtering. Spatial filtering is an important issue, because the background signal is proportional to the detection volume.[11] Additional options are time-gated detection,[12] coherent two-photon excitation,[13−15] or excitation by diode lasers in the red spectral region.[3,16]

So far, three alternative philosophies are known to the authors considering the optical setups currently used for SMD in solution. They have fundamental differences in the spatial detection efficiency (SDE) (see below) and the signal-to-background ratio: (1) the incorporation of ultrasensitve detectors in flow systems for applications in separation science such as microcolumns,[6] microstructures,[8,17] capillaries,[18,19] sheath-flow cells,[12,20,21] and focused microdroplet streams;[22] (2) the use of so-called open detection volume elements, as small as 0.2 fL, within a larger sample solution, using a confocal epi-illuminated fluorescence microscope with a laser beam focused to the diffraction limit;[11,23,24] (3) evanescent field excitation at a quartz−liquid interface.[25−27] Using a certain optical setup, the spatially dependent product of the laser excitation irradiance and fluorescence collection efficiency determines the SDE[28,29] and, hence, the fluorescence burst size of an analyte. (In previous work[28] SDE is called molecular detection efficiency (MDE). MDE might be misleading in this context, since we are dealing with selective quantification of single molecules.) The fluorescence burst size is defined as the number of detected photons associated with a transit of a single molecule through the probe volume. We confine the following discussion to far-field microscopy techniques, since they have the highest SDE due to a simultaneous high excitation and fluorescence collection efficiency.

In contrast to conventional chemical analysis, where at least 10^4 analyte molecules are required to define the peak area and the width of their integrated signal with 1% relative precision,[6] chemical analysis by counting single molecules is not an analogue but a digital process; i.e., a fluorescence burst of size above a certain threshold photon number is considered as one single-molecule event (independent of how far its burst size is above this threshold), provided that simultaneous transitions of multiple molecules can be excluded. After the events of a

* Corresponding author. E-mail: cseidel@gwdg.de.
† Patentanwälte Zenz-Hosbach-Helber & Pa., Huyssen-Allee 58-64, D-45128 Essen, Germany.

S1089-5639(98)00965-7 CCC: $15.00
Published on Web 07/29/1998

single-molecule experiment are defined, quantitative and qualitative analysis can, for example, be performed by a burst size distribution (BSD). A BSD of an experiment is obtained by relating the fluorescence burst sizes to their frequencies within the experiment.

To achieve the detection of all single molecules, in flow-systems the complete sample stream is homogeneously monitored (i.e., detection volume > sample volume) and a defined flow is applied. Thus, the maximum of the resulting BSD is greater than zero and the peak frequency is directly proportional to the fluorescence quantum yield of the dye.[12,30] Yet, the accuracy of SMD (i.e., the number of correctly "digitized" molecules) is determined by the overlap between fluorescence and background signal distributions. The background distribution is caused by fluctuations in the background signal. This distribution has its maximum at zero and decays exponentially.[12,30] Hence, the signal-to-background ratio, which is a relative experimental parameter, and a selected threshold specify the error associated with a measurement (see section 3.2 and refs 22 and 31).

In contrast to flow systems, the relatively small confocal detection volume within a much larger sample volume has an inhomogeneous SDE, which can be well described by a three-dimensional Gaussian distribution[28,29] (see section 3.1.1). This corresponds to the situation that a lot of the randomly diffusing molecules cross near the edges of the open detection volume or miss it entirely. Only a relatively small fraction of molecules traverse the center of the detection volume. Therefore, the resulting BSD of the detected molecules decreases monotonically from zero.[32] In view of the Poisson distributed background signal, this has the consequence that many fluorescence bursts caused by single molecules are too small to be unequivocally identified as a single-molecule event. However, we shall show in this report that in homogeneous assays the open detection volume is very useful to obtain a sample survey based on only those single-molecule events that have a long pathway through the detection volume. Concerning single-molecule spectroscopy, the open detection volume offers several advantages: (1) Due to the small sizes of the detection volumes in the order of 1 fL, excellent signal-to-background ratios larger than 1000 have been achieved for one-photon excitation[11] and two-photon excitation.[14] (2) Because a stationary or scanning volume element can be used to monitor free diffusing or immobilized probe molecules, respectively, in principle any sample compartment, such as biological cells or chemical reactors, can be investigated. (3) The handling, adsorption, and contamination problems of the sample molecules are minimized, because there is no need for an additional flow system.

With respect to the need for fast and low-cost procedures in drug screening, the most notable technique procedure, which uses the open detection volume element, is perhaps fluorescence correlation spectroscopy (FCS).[24,33−35] The autocorrelation analysis of signal traces was pioneered by Wiener[36] as a powerful mathematical tool for noise reduction and data processing. It results in averaging over multiple events. In the last two decades, FCS[37−40] has proved to be a valuable tool to obtain precise statistical characteristics with respect to an average diffusion time, defined, among other things, by the spot size of the laser focus, and to the average molecule number in the detection volume, calculated by the limit of the amplitude of the autocorrelation function at correlation time zero. This is possible without any external calibration standard.

However, there are some limitations for the use of FCS in single-molecule spectroscopy. For very dilute samples with concentrations below 10^{-11} M, the background contributes to a great extent to the total signal. Thus, the conventional number estimations by FCS become erroneous, and a careful background correction is necessary (see section 3.3).[41] In view of the tremendous data reduction of the signal trace by FCS, one has to be aware that in subsequent data analysis the extraction of interesting molecular parameters from FCS data, such as the fluorescence quantum yield, can in some cases be very difficult and involves a complex theory. Thus, binding events monitored by FCS have in practice mainly been analyzed by changes in the characteristic molecular diffusion times. Recent advances using two color fluorescence cross-correlation spectroscopy[35] utilize the amplitude to measure binding events. Furthermore, it is shown by Enderlein and Koellner[42] that FCS is not very useful to characterize individual single molecules "on the fly" via their average characteristic molecular diffusion time, because individual single events and not a statistical average have to be analyzed.

Due to these limitations of FCS, we propose a new strategy to identify and to quantify sample molecules in dilute solution, using a confocal fluorescence microscope and a spectroscopic method denoted as BIFL (burst integrated fluorescence lifetime).[9,12,43] This still enables the experimental advantage of the open volume element. BIFL, which has also been employed by Keller,[12,43] uses pulsed excitation and time-correlated single-photon counting (TCSPC) to measure simultaneously fluorescence intensity and lifetime (see section 2). In contrast to the fluorescence intensity, the lifetime is an absolute parameter and has been successfully used to characterize fluorescent molecules,[2,14] since it is independent of the translational motion, which affects the detection efficiency and, hence, the burst size of the individual single molecule transit. Compared to earlier results,[2] BIFL avoids any integration and averaging of the signal over a certain, fixed time window, since the macroscopic arrival time of each single photon is registered. Thus, the burst analysis is confined to the actual fluorescence photons in the burst, by avoiding the inclusion of extraneous background photons (see section 2).

This paper is organized as follows: In section 3 we derive a closed expression to quantitatively describe a burst size distribution (BSD) in an open volume element and define an error probability for the burst selection. In section 4 we compare BIFL and FCS experiments of two rhodamine dyes characterized by different fluorescence lifetimes. The average number of dye molecules in the sample is obtained, using the theoretical model developed in section 3 and FCS theory, respectively. Furthermore, we demonstrate that BIFL has the opportunity of a complementary data analysis, either by identifying both fluorescent dyes via their specific fluorescence lifetime or by determining the dye specific experimental detection factor in the BSD. In view of the various theoretical estimations of the detection efficiency, Ψ, of an optical setup, we finally note that the analysis of a BSD now offers a direct experimental approach to determine Ψ.

2. Experimental Section

Samples. Three different dye solutions were freshly prepared in water/glycerol (60/40 wt/wt) for single-molecule experiments: solution S(RhB), Rhodamine B (6 pM, Fluka); solution S(Rh6G), Rhodamine 6G (2 pM (Radiant Dyes, Wermelskirchen, Germany)); solution S(MIX), an equimolare mixture (1.5 pM) of the two dyes obtained by mixing the above dye solutions (1 part of S(RhB) and 3 parts of S(Rh6G)). Glycerol was added because of its higher viscosity, which increases the

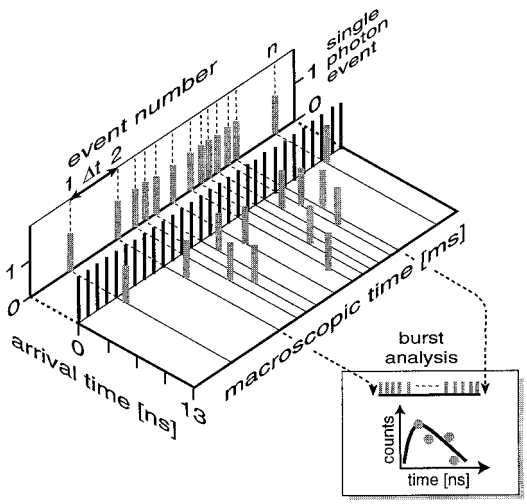

Figure 1. Principle of BIFL spectroscopy with a two-dimensional time measurement and technique for burst selection and fluorescence lifetime determination. (For details, see text.) The time scale of the arrival time axis is determined by the repetition rate of the exciting laser (76 MHz, 13.3 ns).

dwell time in the detection volume. Furthermore, it minimizes the loss of the hydrophobic dye molecules due to adsorption to glass surfaces.

Single Molecule Fluorescence Measurements Using BIFL. Confocal fluorescence detection was performed using a frequency-doubled titanium:sapphire laser (excitation wavelength 522 nm, repetition rate 76 MHz, pulse width 300 fs, Mira 900F (Coherent, Palo Alto, CA)) at an epi-illuminated microscope described previously[14,44] (oil-immersion objective, Fluar 40×, NA = 1.3 oil (Zeiss, Germany)), with a beam-splitter at 530 nm (AHF Analysentechnik, Tübingen, Germany), a 80 μm pinhole, and a dichroic band-pass emission filter (HQ 582/50 nm (AHF Analysentechnik)). The samples were measured in microscope slides with small depressions (100 μL) under cover glasses. The fluorescence signal of the sample was detected by an avalanche photodiode (AQ 151 (EG&G, Vaudreuil, Quebec, Canada)) and registered by a newly developed BIFL module (see below).

The BIFL technique records two types of information for each detected photon (Figure 1): (I) The time lag, Δt, to the preceding signal photon (gray lines) as a measure of the macroscopic detection time of the events in the experiment (millisecond time scale) is recorded. This allows for a specific and photon-exact fluorescence burst selection. (II) The arrival time of the signal photon relative to the exciting laser pulse (black line), measured by time-correlated single-photon counting (picosecond−nanosecond time scale) is recorded. The arrival times of all photons in a selected fluorescence burst are combined in a histogram (see burst analysis in Figure 1), and a fluorescence lifetime is calculated by a maximum likelihood estimator (see section 3.4).

The BIFL module consists of a time-correlated single-photon counting unit with NIM modules (constant fraction discriminator Tennelec TC 454 and time-to-amplitude converter Tennelec TC 862 (Eurisys Messtechnik, Mainz, Germany), analog−digital converter 7423 UHS-S (Silena, Milano, Italy)), and a self-designed alternating counterboard, which is triggered by the NIM analog−digital converter output signal. This measures the time lag, Δt, between two detected photons. For each event, both types of temporal information are stored on a computer interfaced with a PC-board (ATDIO32F (National Instruments)).

Multiplexing the detector signal and using a real-time correlator card (ALV-5000/E (ALV, Langen, Germany)), the BIFL-measurement was checked independently and simultaneously by FCS. The radial and axial $1/e^2$ radius of the detection volume, $\omega_0 = 0.62$ μm and $z_0 \approx 12.4$ μm, were determined from FCS measurements of Rhodamine 6G (Rh6G) in pure water with a characteristic diffusion time of $\tau_D = 0.32$ ms, assuming a diffusion constant of $D = 3 \times 10^{-6}$ cm^2 s^{-1}.[45] This corresponds to a detection volume of $V = 2.65 \times 10^{-14}$ L. The sample was excited at a power of $P = 915$ μW, which is equivalent to a quasi-continuous focal excitation irradiance of $I_0 = P/(0.5\pi\omega_0^2) = 1.5 \times 10^5$ W/cm^2.

3. Theory

3.1. Burst Size Distribution (BSD) in an Open Detection Volume. The aim of this section is to derive a quantitative expression for a burst-size distribution (BSD) of a "single-molecule" experiment, using an open detection volume element in solution at a given low concentration of a fluorescent sample. Thereby, it is important for us to use simple mathematical procedures that can easily be programmed on a PC. The BSD is subsequently determined from the BIFL data, by analyzing the frequency of bursts containing a total number of detected photons, C_t (burst size). Thus, we define the probability, $P(C_t,N_{av})$, of detecting a total number of photons, C_t, in a fluorescence burst at a given average molecule number, N_{av}, in the detection volume. Taking into account that a burst might be caused by more than one molecule, this probability is influenced by three parameters. The first parameter regards the probability, $P_1(C_t)$, to detect C_t photons in a burst caused by a single molecule. It is determined by individual experimental and molecular parameters. The second parameter takes into account that the probability, $P_1(C_t,t)$, of detecting C_t photons emitted by a single molecule also depends on the dwell time t in the detection volume. Thus, it is advantageous to assume a distribution, $Pt_1(t)$, of dwell times, t, for a single-molecule transit, leading to the overall density function, $P_1(C_t)$, defined by the integral over all dwell times, t.

$$P_1(C_t) = \int_0^\infty P_1(C_t,t)Pt_1(t)\,dt \qquad (1)$$

The third parameter must consider the probability, $Pm_n(N_{av})$, that more than one molecule (i.e., n molecules) may diffuse through the detection volume which are separated less than the mean transit time and, thus, produce a single unresolved fluorescence burst due to a multimolecule (n-molecule) event. Hence, the probability, $P_n(C_t)$, to detect C_t photons for a multimolecule event within a single burst is given by iterative convolution of the overall density function, $P_1(C_t)$, of single-molecule events. We obtain for a two-molecule event

$$P_2(C_t) = P_1(C_t) \otimes P_1(C_t) = \sum_{i=1}^{C_t-1} P_1(C_t - i)P_1(i) \qquad (2)$$

and for a multimolecule event

$$P_n(C_t) = P_{n-1}(C_t) \otimes P_1(C_t) = \sum_{i=1}^{C_t-1} P_{n-1}(C_t - i)P_1(i) \qquad (3)$$

The final expression of the density function, $P(C_t,N_{av})$, that a single fluorescence burst contains C_t detected photons is then given by the sum over all possible n-molecule events.

$$P(C_t,N_{av}) = Pm_1(N_{av})P_1(C_t) + Pm_2(N_{av})(P_1(C_t) \otimes P_1(C_t)) + ... = \sum_{n=1}^{\infty} Pm_n(N_{av})P_n(C_t) \quad (4)$$

Following the above guidelines, we subsequently calculate the three individual parameters, $P_1(C_t,t)$, $P_1(C_t)$, and $Pm_n(N_{av})$. Let us first find $P_1(C_t,t)$ for a single, randomly diffusing, fluorescent molecule under a given, space-dependent excitation irradiance, $I(\vec{r})$ (W/cm^2). Thereby, we compare the approaches reported by Rigler and Mets,[32] Qian,[46] and Enderlein et al.[47] and for the first time consider triplet kinetics and saturation of the fluorescence as well as of the detection electronics.

3.1.1. Density Function $P_1(C_t,t)$. *Photon Emission as a Stochastic Process.* Because the diffusion and the fluorescence detection of a single molecule can be assumed as a random process, the probability $P_1(C_t,t)$ is described by a Poisson distribution (eq 5) defining the shot noise.[46,48] $C_{t,av}(t)$ is the

$$P_1(C_t,t) = \frac{C_{t,av}(t)^{C_t}}{C_t!} \exp(-C_{t,av}(t)) \quad (5)$$

mean number of fluorescence photons detected in the total detection volume within the dwell time interval t. The value of $C_{t,av}(t)$ is influenced by the space-dependent spatial detection efficiency (SDE), Δ. The spatial detection efficiency, Δ, within the detection volume is defined by the irradiance profile of the focused laser beam, $I(\vec{r})$, and by the collection efficiency of the optical setup.[28,29]

As a first approximation, Δ may be described by a constant value over the detection volume, V. Hence, the mean photon number, $C_{t,av}(t)$, is linearly related to the dwell time, t, and the applied irradiance, I, if triplet kinetics and fluorescence saturation are neglected.

$$C_{t,av}(t) = gIt \qquad g = \Psi\Phi_F\sigma_{01}(\lambda_{ex})\gamma \quad (6)$$

The experimental detection factor, g, is defined by the detection efficiency of the optical setup, Ψ, the fluorescence quantum yield of the dye, Φ_F, the dye specific absorption cross section, $\sigma_{01}(\lambda_{ex})$, at the excitation wavelength λ_{ex}, and the inverse photon energy, $\gamma = \lambda_{ex}/hc_1$ (h is the Planck constant and c_1 the velocity of light).

However, a more detailed description[28,29] uses a three-dimensional Gaussian distribution for the spatial detection efficiency, Δ.

$$\Delta(x,y,z) \propto I(x,y,z) = I_0 \exp(-2(x^2 + y^2)/\omega_0^2) \exp(-2z^2/z_0^2) \quad (7)$$

I_0 is the irradiance in the focal plane of the laser beam ($z = 0$) and ω_0 and z_0 are the $1/e^2$ radii of the laser beam in the radial (x, y) and axial (z) directions, respectively. In this case, one should calculate the mean number of emitted photons, $C_{t,av}(t)$, for a certain dwell time, t, by a sum over all short time intervals, dt_{sh}, where the molecule is in volume shells of equal spatial detection efficiency (eq 8).

$$C_{t,av}(t) = \int_0^t gI(t_{sh})\, dt_{sh} \quad (8)$$

In general, it is impossible to find an analytical solution for this problem. Enderlein et al.[30,47] applied a numerical solution using a Monte Carlo method, which randomly samples molecule trajectories calculated by path integrals running over all possible positions, $\vec{r} = (x,y,z)$. Because the burst size statistics averages over many single-molecule events, we combine the eqs 5−8 and prefer to calculate the density function $P_1(C_t,t)$ for a certain dwell time, t, by considering an average number of emitted photons detected from all possible positions, $\vec{r} = (x,y,z)$, in the detection volume, V (eq 9).

$$P_1(C_t,t) \propto \int_V \frac{(gI(\vec{r})t)^{C_t}}{C_t!} \exp(-gI(\vec{r})t)\, dV = K_{ST}\int_0^{\infty} \frac{(gI(r)t)^{C_t}}{C_t!} \exp(-gI(r)t)\, r^2\, dr \quad (9)$$

Equation 9 can be solved by numerical integration using spheric coordinates ($r^2 = (x^2 + y^2 + z^2)$) and by defining a normalization constant, K_{ST}.

Burst Size Frequencies and Irradiance Shells. As an alternative to eq 9, Rigler and Mets[32] proposed an analytical expression for $P_1(C_t,t)$. It is based on the idea that the free diffusing molecule can be found at any point of space with equal probability. Hence, the probability to find a fluorescence burst of a certain size is proportional to the volume of the corresponding constant-irradiance shell in the detection volume element.

To calculate the volume of the shell, ∂V, for an irradiance increase, ∂I, within the boundaries I and $I + \partial I$, the two space dependent parameters V and I must be combined. If we use the three-dimensional elliptical Gaussian distribution in V (eq 7) with the half-axes $r_x = r_y = r_{x,y}$ and r_z, only one variable, $r_{x,y}$, is necessary to describe the space dependence of the detection volume, $V = {}^4/_3\pi r_{x,y}{}^2 r_z = {}^4/_3\pi r_{x,y}{}^3(z_0/\omega_0) = V(r_{xy})$, in eq 10 and of the irradiance, $I(r_{x,y}) = I_0 \exp(-2r_{x,y}{}^2/\omega_0{}^2)$, in eq 11.

$$\frac{\partial V(r_{x,y})}{\partial r_{x,y}} = 4\,\pi r_{x,y}{}^2(z_0/\omega_0) \quad (10)$$

$$\frac{\partial r_{x,y}}{\partial I} = -\frac{\omega_0}{\sqrt{8}} \frac{\sqrt{\ln(I_0/I)}}{I} \quad (11)$$

Because the density function $P_1(C_t,t)$ is proportional to the volume of the corresponding constant-irradiance shell, ∂I, in the detection volume element, ∂V, and, hence, to $\partial V/\partial I$, we finally use the eqs 6 and 8 to calculate the total number of detected fluorescence photons, C_t, in the shell of the irradiance $I + \partial I$ ($C_t(I) = gIt$; $\partial V/\partial I = gt(\partial V/\partial C_t)$). We normalize by the constant K_{IS} (eq 12).

$$P_1(C_t,t) \propto \left|\frac{\partial V}{\partial I}\right| = \left|\frac{\partial V}{\partial r_{x,y}} \frac{\partial r_{x,y}}{\partial I}\right| = \frac{\pi\omega_0{}^2 z_0}{\sqrt{2}} \frac{\sqrt{\ln(I_0/I)}}{I} = K_{IS} \frac{\sqrt{\ln(gI_0t/C_t)}}{C_t} \quad (12)$$

Considering the BSD of single-molecule events with a certain dwell time, $t = 1$ ms, the equivalence of both approaches (eq 9 (open circles) and eq 12 (solid line)) to calculate the density function $P_1(C_t,t)$ is demonstrated in Figure 2A, where $P_1(C_t,t)$ is plotted as a function of the total number of detected burst photons, C_t.

Within the region of interest both density functions $P_1(C_t,t)$ are identical. However, eq 12 has the advantage of a direct analytical solution and will be used for subsequent analysis.

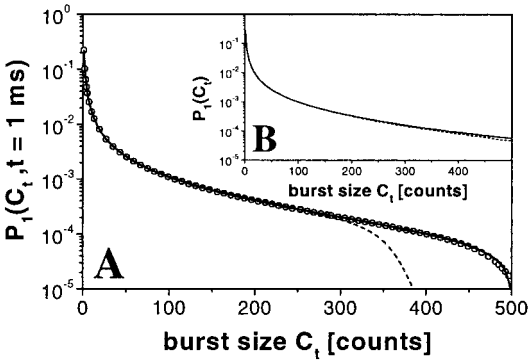

Figure 2. (A) Simulated probability density function, $P_1(C_t,t)$, with a single fixed dwell time, $t = 1$ ms, as a function of the number of detected fluorescence photons, C_t (counts) caused by one single molecule diffusing through the detection volume. $P_1(C_t,t)$ is shown for two cases: (1) neglecting triplet kinetics and fluorescence saturation ($C_{t,av}$ (eqs 6 and 8)); (2) considering triplet kinetics and fluorescence saturation ($C_{t,av-S}$ (eq 13)). The different curves are calculated by the numerical approach of a stochastic process (average count rate approach) ($C_{t,av}$, eq 9 (open circles); $C_{t,av-S}$, eq 14 (dashed line)) and by the analytical approach of constant-irradiance shells ($C_{t,av}$, eq 12 (solid line); $C_{t,av-S}$, eq 15 (dashed line)). The used parameters are $\tau = 2.3$ ns, $\Phi_F = 57.5\%$, $\sigma_{01}(522\text{ nm}) = 1.4 \times 10^{-16}$ cm^2, $k_{ISC} = 8 \times 10^5$ s^{-1}, $k_T = 4 \times 10^5$ s^{-1}, and $\Psi = 1.5\%$. (B) Simulated probability density function, $P_1(C_t)$ (eq 1), as a function of the number of detected fluorescence photons, C_t (counts), caused by one single molecule diffusing through the detection volume. A dwell time distribution, $Pt_1(t)$ with a mean transit time of $t_t = 1.2$ ms is used (eq 17). Regarding the analytical approach of the eqs 12 and 15, two cases are considered: Equation 12 ($C_{t,av}$) neglecting (solid line) and eq 15 ($C_{t,av-S}$) considering (dotted line) triplet kinetics and fluorescence saturation. The same parameters were used as in Figure 2A.

Triplet Kinetics, Fluorescence Saturation, and Photobleaching. In our case, a focal excitation irradiance $I_0 = 1.5 \times 10^5$ W/cm^2 is applied. Thus, the population of the triplet state and fluorescence saturation should be taken into account; i.e., the photon number, $C_{t,av}(t) = gIt$ (eqs 6 and 8), for a certain dwell time, t, is no more proportional to the irradiance, I, but levels off at higher irradiances. However, photobleaching can be neglected, since the average total number of emitted fluorescence photons of a single molecule transit is not affected by photobleaching at our experimental conditions of $I_0 = 1.5 \times 10^5$ W/cm^2 and of a mean transit time, $t_t = 1.2$ ms (eq 17 and section 4) (see Figure 5 of ref 49).

Therefore, a modified expression, $C_{t,av-S}(t)$ (eq 13), for the mean photon number is calculated, which assumes that the

$$C_{t,av-S}(t) = \Psi\Phi_F(1/\tau)S_{1eq}(I)t \qquad (13)$$

$$S_{1eq}(I) = \frac{(\sigma_{01}(\lambda_{ex})\gamma I)k_T}{(\sigma_{01}(\lambda_{ex})\gamma I)(k_{ISC} + k_T) + k_T/\tau}$$

emission of a fluorescence photon is proportional to the probability, $S_{1eq}(I)$, of a dye molecule to be in the first excited singlet state, S_1, at a certain excitation irradiance, I. For the probability S_{1eq}, we assume an electronic energy diagram of a dye molecule consisting of three electronic levels (electronic ground state, S_0, first excited singlet state, S_1, and lowest excited triplet state, T_1) with the fluorescence lifetime, τ, and the rate constants for intersystem crossing and for depopulation of the triplet state, k_{ISC} and k_T, respectively.[49] Taking the modified expression of $C_{t,av-S}(t)$ (eq 13) and introducing normalization constants, K_{ST-S} and K_{IS-S}, respectively, the density function $P_1(C_t,t)$ regarding triplet kinetics and fluorescence saturation can be calculated in analogy to eq 9 (eq 14) and eq 12 (eq 15).

$$P_1(C_t,t) = K_{ST-S}\int_0^\infty \frac{(\Psi\Phi_F(1/\tau)S_{1eq}(r)t)^{C_t}}{C_t!} \exp(-\Psi\Phi_F(1/\tau)S_{1eq}(r)t)\, r^2\, dr \qquad (14)$$

$$P_1(C_t,t) = K_{IS-S}\frac{a_1 t}{a_1 t - a_2 C_t}\frac{\sqrt{\ln[(I_0 a_1 t - I_0 a_2 C_t)/(a_3 C_t)]}}{C_t} \qquad (15)$$

$$a_1 = [\Psi\Phi_F(1/\tau)k_T(\sigma_{01}(\lambda_{ex})\gamma)] \quad a_2 = [(k_{ISC} + k_T)(\sigma_{01}(\lambda_{ex})\gamma)] \quad a_3 = (1/\tau)k_T$$

In the same way as eqs 9 and 12, the alternative approaches of eqs 14 and 15 also lead to equivalent results. Thus, the both approaches (average count rate or constant-irradiance shells) are always equivalent, independent of the applied fluorescence−irradiance relation (eq 6 or 13). For the case of a dwell time of $t = 1$ ms, differences between the density functions $P_1(C_t,t)$ for $C_{t,av-S}(t)$ (dotted line in Figure 2A) or $C_{t,av}(t)$ (open circles and solid line), which neglects triplet kinetics and fluorescence saturation, are only detectable for high photon numbers, C_t. In these cases, the molecule spends a long time in the focal center of maximum irradiance, where the influence of triplet population and fluorescence saturation is marked.

The simulated BSDs show that under our conditions it is sufficient to use the approach of eq 12 for subsequent analysis.

Saturation of the Detection Electronics. The performance of the detection electronics of our BIFL module is limited by the dead-time of the NIM modules and by the computer data acquisition, which allow count rates of up to 137 kHz. Because well-defined bursts (i.e., bursts caused by single-molecule transits through the center of the detection volume (see section 3.1.2)) are selected, the mean count rate per detected fluorescence burst is constant. This is consistent with the result that the plot of the burst size, C_t, versus the individual transit times, t, is linear (data not shown). Therefore, it is useful to introduce a detection efficiency of the detection electronics, Ψ_{electr}. Due to the constant count rate per burst, Ψ_{electr} is supposed to be constant for every burst. The experimental detection factor, g (eq 6), should then be extended by Ψ_{electr}.

$$g = \Psi\Psi_{electr}\Phi_F\sigma_{01}(\lambda_{ex})\gamma \qquad (16)$$

Comparing the mean count rates per molecule (cpm) of the different dye solutions at our experimental conditions (see section 2) recorded by BIFL (maximum possible count rate 137 kHz) and by the correlator card (FCS, maximum possible count rate 125 MHz), we determined a value of $\Psi_{electr} = 0.79$ for all dye solutions (e.g., S(Rh6G): cpm(BIFL) = 85 kHz, cpm(FCS) = 108 kHz).

3.1.2. Density Distribution of Dwell Times *Pt(t)*. The trajectories of molecules through an open detection volume element undergoing free diffusion with a diffusion coefficient D can be described by two border cases:[23,50] (1) boundary recrossing motions result in multiple small bursts, whereas (2) traversing motions through the entire three-dimensional detection volume with the radius ω_0 produce well-defined bursts with a mean transit time $t_t = \omega_0^2/(3D)$.[33] We select only well-defined bursts, because a certain minimum number of fluorescence photons is needed for analysis, due to several reasons discussed below in more detail: (1) A decision has to be made whether a certain burst has been caused by a passing molecule or is due to background fluctuations. (2) The variance of a single-molecule identification via characteristic fluorescence lifetimes

is inversely proportional to the number of analyzed fluorescence photons. (3) The dwell times of central single-molecule transits can be well described by an exponential distribution, $Pt_1(t)$.[50]

$$Pt_1(t) = 1/t_t \exp(-t/t_t) \tag{17}$$

In the case of the distribution of experimentally determined dwell times, t, multimolecule events have to be considered, and thus the probability, $Pm_n(N_{av})$, of n-molecule events (see section 3.1.4) has to be taken into account. The experimentally observed mean burst duration, t_B (apparent average transit time), is simply given by a weighted sum of mean transit times ($n\ t_t$).

$$Pt_m(t) = 1/t_B \exp(-t/t_B)$$
$$t_B = \sum_{n=1}^{\infty} (n\ t_t) Pm_n(N_{av}) \tag{18}$$

3.1.3. Overall Density Function $P_1(C_t)$. According to eq 1, the overall density function, $P_1(C_t)$, of single molecule events is calculated by integrating the product of the probability distributions $Pt_1(t)$ and $P_1(C_t,t)$ over all dwell times, t. This function $P_1(C_t)$ is shown in Figure 2B for the two different cases, either neglecting (eq 12, solid line) or considering (eq 15, dotted line) triplet kinetics and fluorescence saturation, using parameter values which are characteristic for rhodamine dyes.[49] Comparing both cases, saturation effects only result in a slight difference for very high photon numbers, C_t, larger than 300 photons. Because our largest detected photon number was lower, the influence of triplet kinetics and fluorescence saturation is negligible in subsequent analysis. Hence, it is most convenient to analyze all BSDs of this report using eq 12.

3.1.4. Probability of Multimolecule Events $Pm_n(N_{av})$. The probability, $P_n^e(t,N_{av},t_t)$, that n molecules enter the detection volume during the time t is described by a Poisson distribution and depends on the sample concentration with the corresponding average molecule number in the detection volume, N_{av}, on the mean transit time of a single molecule, t_t, and on the observation time window, t.[51]

$$P_n^e(t,N_{av},t_t) = \frac{(N_{av}(t/t_t))^n}{n!} \exp(-N_{av}t/t_t) \tag{19}$$

With the definition of a mean entering time, $t_e = t_t/N_{av}$, the probability of no, $P_0^e(t) = \exp(-t/t_e)$, and the probability of one entry, $P_1^e(t) = t/t_e \exp(-t/t_e)$, during the time interval t can be evaluated.

If one assumes a mean constant transit time, $t = t_t$, for each single-molecule transit, the probability $Pm_n(N_{av})$, that a fluorescence burst might be caused by n molecules yielding an unresolved burst is given by a product of probabilities which correspond to a sequence of n single-molecule events;[47] i.e., a certain burst is described by the probability that n single molecules enter the detection volume successively, being separated by times less than t_t, and by the probability of having no entry before and after the burst.

$$Pm_n(N_{av}) \propto P_0^e(t_t)\left[\prod_{j=1}^{n-1}\int_0^{t_t}\frac{dt_j}{t_e}\exp(-t_j/t_e)\right]P_0^e(t_t)$$
$$= \frac{\exp(-2N_{av})(1-\exp(-N_{av}))^{n-1}}{\sum_{n=1}^{\infty}\exp(-2N_{av})(1-\exp(-N_{ev}))^{n-1}} \tag{20}$$

We note that $Pm_n(N_{av})$ is normalized ($\sum_{n=1}^{\infty} Pm_n(N_{av}) = 1$), since we consider selectively fluorescence bursts and not the total signal including background.

3.1.5. Absolute Burst Size Statistics $\beta(C_t,N_{av})$. So far, we have derived the density function, $P(C_t,N_{av})$, to calculate the probability that C_t photons are detected in a burst. However, a BIFL experiment contains a total number of fluorescence bursts, B_{mes}, within the measurement time, t_{mes}. Bursts which are above a certain threshold and have a minimum number of fluorescence photons (see below) are selected. This sample survey is analyzed to determine the frequency of bursts, $\beta(C_t,N_{av})$, containing a total number of detected photons, C_t (burst size). For a statistical analysis, a relation between the experimentally obtained individual burst size histograms, $\beta(C_t,N_{av})$, and the theoretical, normalized density function, $P(C_t,N_{av})$, is established through B_{mes}.

$$\beta(C_t,N_{av}) = B_{mes}\, P(C_t,N_{av}) \tag{21}$$

Because not all bursts can be analyzed due to background fluctuations, the total number of fluorescence bursts, B_{mes}, within t_{mes} can in principle not exactly be determined. Thus, B_{mes} must be calculated through its relation to the total time of fluorescence, t_F, within the experimentally determined measurement time, t_{mes}. The total time of fluorescence, t_F, is either given by the product of t_{mes} with the probability of detecting any molecule in the detection volume, $(1 - \exp(-N_{av}))$, or by the product of B_{mes} with the average burst duration, t_B (see eq 18).

$$t_{mes}(1-\exp(-N_{av})) = t_F = B_{mes}\, t_B \tag{22}$$

The analysis of the obtained BSD, $\beta(C_t,N_{av},g)$, by eq 23 (considering also eqs 1, 4, 12, 17, and 20) allows one to determine the parameters of interest, N_{av}, and the detection factor g.

$$\beta(C_t,N_{av},g) = P(C_t,N_{av},g)(1-\exp(-N_{av}))\frac{t_{mes}}{t_B} \tag{23}$$

To conclude, we have developed a theory which quantitatively describes BSDs, β, in open detection volume elements. The analysis of β now provides direct experimental access to the detection efficiency, Ψ, of the confocal optical setup. Ψ was formerly estimated by standard factors.[21] Furthermore, it also allows us to determine the average number of molecules in the detection volume, N_{av}, complementary to fluorescence correlation spectroscopy (FCS).

3.2. Burst Selection Criteria. If fluorescence bursts monitored in a BIFL experiment should be selected for analysis in a BSD, the question has to be answered whether a certain burst has been caused by a passing molecule or is due to background fluctuations. Hence, selection criteria based on a certain error probability, α, must be established. These selection criteria define a threshold parameter to select single-molecule events. We will show, in the following, that the specific time information, Δt, of the BIFL data provides an elegant way to define a statistical basis.

The time lag between the arrival time of subsequent background photons, Δt, is exponentially distributed with a mean

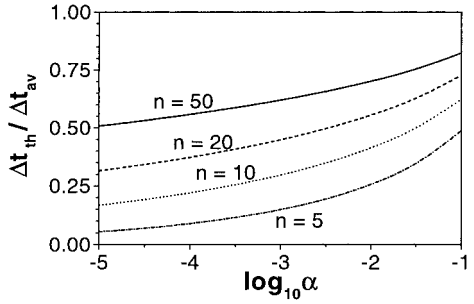

Figure 3. Error probability, α (eq 26), of a false burst identification by selecting events caused by background fluctuations as a function of the ratio $\xi = \Delta t_{th}/\Delta t_{av}$. α is given for the case of smoothing the data over $n = 5$, 10, 20, and 50 photons.

time lag, Δt_{av} (eq 24). This is equivalent to stating that the

$$P(\Delta t) = \frac{1}{\Delta t_{av}} \exp(-\Delta t/\Delta t_{av}) \tag{24}$$

number of background photons per time unit follows a Poisson distribution, $P(\Delta t)$. As a consequence, the time lag between successive background photons, Δt, fluctuates extremely.

Because all efficient statistical procedures rely on discriminating between signal and background, the data were smoothed by calculating the arithmetic mean, $\Delta t_{sm}(n) = 1/n\sum_{i=1}^{n}\Delta t_i$, over n lag times, Δt_i. The resulting background distribution, $P(\Delta t_{sm}(n))$, is obtained by n times successive convolution of eq 24 and given by the gamma distribution, $P(\Delta t_{sm}(n))$, with a mean time lag, Δt_{av}.

$$P(\Delta t_{sm}(n)) = \frac{(n/\Delta t_{av})^n}{(n-1)!}\Delta t^{n-1} \exp(-n\Delta t/\Delta t_{av}) \tag{25}$$

In view of an appropriate burst selection with a low threshold, Δt_{th}, one can calculate the probability that a burst, i.e., a dip in the BIFL trace, has been caused by background photons. This is equal to the probability of n background photons having an arithmetic mean $\Delta t_{sm}(n) \le \Delta t_{th}$; i.e., $P(\Delta t_{sm}(n) \le \Delta t_{th}|\Delta t_{av})$ is the probability, α, of a false identification by selecting events caused by background fluctuations.

$$\begin{aligned} P(\Delta t_{sm}(n) \le \Delta t_{th}|\Delta t_{av}) &= \int_0^{\Delta t_{th}} \mathrm{d}(\Delta t)\frac{(n/\Delta t_{av})^n}{(n-1)!}\Delta t^{n-1} \exp(-n\Delta t/\Delta t_{av}) \\ &= \int_0^{\Delta t_{th}/\Delta t_{av}} \mathrm{d}\xi\frac{n^n}{(n-1)!}\xi^{n-1} \exp(-n\xi) = \alpha \end{aligned} \tag{26}$$

Using the relative variable $\xi = \Delta t_{th}/\Delta t_{av}$, the threshold can now be treated as a dimensionless parameter which is equivalent to the ratio of the threshold to the mean background signal. In this way, an exact value for a threshold, Δt_{th}, can be set, which corresponds to a certain error probability, α, at a given mean background time lag, Δt_{av}. We note, that smoothing of the data affects the density distribution of $\Delta t_{sm}(n)$ and, therefore, results in different error probabilities, α. The effect of smoothing on α is demonstrated in Figure 3, considering typical example values for smoothing with $n = 5$, 10, 20, and 50.

3.3. Fluorescence Correlation Spectroscopy (FCS). We used fluorescence correlation spectroscopy (FCS)[37−40] as an alternative statistical tool to obtain additional experimental values of the average molecule number, N_{av}, in the detection volume and the dimensions of the detection volume (e.g., spot size of the laser focus). The normalized autocorrelation function, $G(t_c)$, with the correlation time, t_c, allows for the analysis of fluctuations in the fluorescence signal, $\delta F(t)$, about an average value, $\langle F(t)\rangle$ ($F(t) = \langle F(t)\rangle + \delta F(t)$) (eq 27).

$$G(t_c) = \frac{\langle F(t)F(t+t_c)\rangle}{\langle F(t)\rangle^2} = 1 + \frac{\langle \delta F(t)\delta F(t+t_c)\rangle}{\langle F(t)\rangle^2} \tag{27}$$

If a spatial three-dimensional Gaussian distribution (eq 7) of the detected fluorescence is assumed,[28,52] and if triplet kinetics and translational diffusion through the detection volume, V, are the only noticeable processes of the fluorescent molecules which cause the fluctuations, $\delta F(t)$, $G(t_c)$ is given by eq 28.[45] T_{1eq} is

$$G(t_c) = 1 + \frac{(1 - I_B/I_S)^2}{N_{av}(1 - T_{1eq})}[1 - T_{1eq} + T_{1eq}\exp(-t_c/t_T)] \left(\frac{1}{1 + (t_c/\tau_D)}\right)\left(\frac{1}{1 + (\omega_0/z_0)^2(t_c/\tau_D)}\right)^{1/2} \tag{28}$$

the average fraction of molecules in the excited triplet state, T_1, with a triplet correlation time, t_T. $\tau_D = \omega_0^2/4D$ is the characteristic time for diffusion of the fluorescent molecules through the detection volume, V, and related to the radial $1/e^2$ radius of V, ω_0, via the translational diffusion coefficient of the fluorescent molecules, D. The limit of the amplitude of the time-dependent term, $G(t_c = 0)$, is equivalent to the normalized variance of the fluorescence (second-order central moment of light intensity).[46,48,53] $G(t_c = 0)$ is given by the inverse of the average molecule number in the detection volume without the triplet population, $1/[N_{av}(1 - T_{1eq})]$. However, it is crucial in single-molecule experiments to correct for the decrease of the amplitude, $G(t_c = 0)$, caused by background signal. This is accomplished by considering the ratio of the background flow, I_B, to the total signal flow, I_S ($I_S = F + I_B$), and including the correction factor, $f_c = (1 - I_B/I_S)^2$, in the numerator of eq 28.[41]

3.4. Identification of Single Molecules. Because the number of detected fluorescence photons in SMD is small, we used the statistically most efficient pattern recognition technique[54] to determine the fluorescence lifetime, τ, of a certain experimental data set, *Pd*, given in a histogram with only a few photons.[14] The analysis is based on a maximum-likelihood estimator (MLE)[55] and the multinomial distribution.[56−58] It is described in more detail in ref 14. The fluorescence data, *Pd*, obtained by time-correlated single-photon counting are accumulated in $k = 120$ channels of a finite nanosecond measurement window, $T = 13.3$ ns. In the following we compare the experimentally obtained probability, *Pd*, with a synthetically generated signal pattern, *Pp*.

In our experiments each signal decay pattern, *Pp*, may contain variable contributions of fluorescence, *Pf*, with a characteristic fluorescence lifetime, τ, and background signal, *Pir*, due to the Raman signal of the solvent. Therefore, the signal decay pattern, $Pp_i(\tau, T, k, \gamma, Pir)$, in the channel i is given by the normalized sum of variable fractions of background, γ, and fluorescence, $1 - \gamma$.

$$Pp_i(\tau,T,k,\gamma,Pir) = \gamma\frac{Pir_i(T,k)}{\sum_{i=1}^{k} Pir_i(T,k)} + (1-\gamma)\frac{Pf_i(\tau,T,k)}{\sum_{i=1}^{k} Pf_i(\tau,T,k)} \tag{29}$$

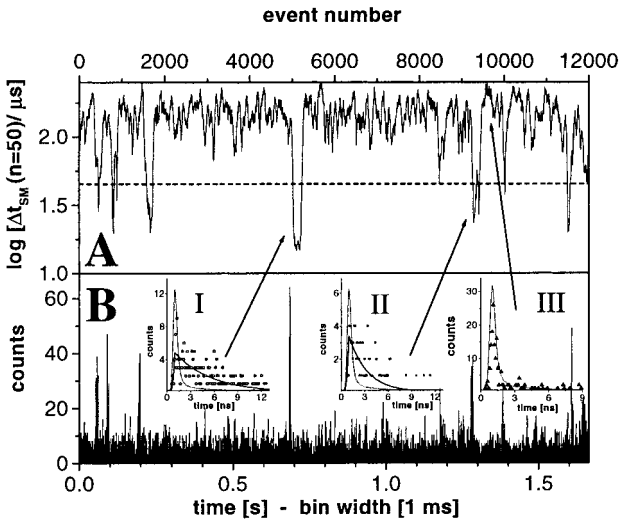

Figure 4. Two equivalent BIFL representations of a time-dependent signal trace of S(MIX). (A) Time lag, $\Delta t_{SM}(50)$, between consecutive photons of the smoothed data (averaged for $n = 50$ originally recorded lag times, Δt) versus the signal event number, and threshold value, Δt_{th}, for the subsequent burst selection ($\Delta t_{th} = 45$ μs, dashed line). (B) Multichannel scaler (MCS) trace with a bin width of 1 ms calculated from the Δt trace of (A) versus the macroscopic measurement time of the experiment. The different *x*-axes of (A) and (B) reveal slight distortions in the position of related fluorescence bursts. Insets: Two typical fluorescence decays (I and II) and background signal (III) obtained from photons of the same measurement indicated by arrows in (A): fluorescence decay (open circles, full circles, and triangles), instrument response function (dotted line), and fit (straight line) by MLE [τ(I) = 3.9 ns, τ(II) = 2.0 ns].

The probability, Pf_i, of finding a fluorescence count in channel i for a single-exponential decay is generated in two steps (eq 30): (1) u channels of the density function of the instrument

$$Pf_i(\tau,T,k) = \sum_{\upsilon=0}^{\theta}\left(\sum_{i=0}^{\min(i,u)} Pir_j \exp\left(\frac{-(i-j)T}{\tau k}\right)\right)_{i+\upsilon W} \qquad (30)$$

response function, *Pir* (identical to the background due to scattered laser light), are convoluted with the exponential distribution for a given fluorescence lifetime, τ. (2) Because the repetition rate, $f = 76$ MHz (13.3 ns), of the pulsed excitation laser is high compared to the fluorescence lifetime, τ, of a fluorescent dye (e.g., S(Rh6G): $\tau = 3.7$ ns), the possibility that a dye could have been excited by a previous pulse has to be considered (for the above example 2.8%). Hence, Pf_i is calculated by a sum over several pulses, θ, preceding the fluorescence photon with the channel increment, $W = k/(Tf)$.

The MLE (eq 31) compares the experimental photon density function, *Pd*, which is given by the number of detected photons

$$2I_r^* = \frac{2}{k-1-f}\sum_{i=1}^{k} c_i \ln\left(\frac{c_i}{C_t Pp_i(\tau,T,k,\gamma,Pir)}\right) \qquad (31)$$

in channel i, c_i, of the total signal, C_t (i.e., burst size), and the synthetic pattern, $Pp_i(\tau,T,k,\gamma,Pir)$, by varying the two parameters γ and τ. The fit is judged by calculating a quality parameter (denoted as reduced $2I_r$*) for the various steps of optimization. On the basis of a minimum reduced $2I_r$*,[59] an optimal pattern, $Pp_i(\tau,T,k,\gamma,Pir)$, for this two-dimensional surface of the fitted parameters, γ and τ (i.e., $f = 2$), is determined.

4. Results and Discussion

In this section, we will show the ability of time-resolved single molecule detection in combination with our BIFL technique to identify and to quantify different single molecules.

Burst Selection. The first step in analyzing a single molecule experiment is to distinguish between fluorescence and background. This can nicely be realized using the macroscopic time, Δt, information of a BIFL measurement (Figure 1). The time lag, Δt, between two consecutive detected background photons is very large, whereas fluorescence photons emitted during a dye transit cause a photon burst and thus have a small time lag, Δt. Figure 4 shows two equivalent representations of a BIFL measurement of the mixed dye solution, S(MIX). The Δt values enable one to calculate a conventional multichannel scaler (MCS) trace in any desired bin width. This is accomplished by integration over those detected photons whose sum of Δt values corresponds to the selected bin width. A single molecule transit through the detection volume of our setup causes a fluorescence burst in the MCS trace (Figure 4B), which corresponds to a drop in the Δt trace (Figure 4A). It is important to note that the Δt values are plotted for the event number as originally recorded in a BIFL measurement and not versus time. In contrast, the calculated MCS trace is plotted for the measurement time. This reveals two different *x*-axes of both plots and results in slight distortions of the position of the bursts. The presented Δt trace is smoothed over 50 photons ($n = 50$) according to eq 25.

The mean background count rate of 6 kHz is equivalent to a mean time lag between background photons of $\Delta t_{av} = 170$ μs. A maximum number of fluorescence photons of $C_t \approx 200$ is detected (compare Figure 7A/B). Using the above parameter and a characteristic diffusion time of $\tau_D = 0.9$ ms obtained by FCS in this solvent mixture, a signal-to-background ratio of S/B ≈ 37 is calculated.[11,14] Compared to other values reported for confocal detection, the obtained S/B value is rather small. However, besides the saturation effects of our detection electronics, $\Psi_{electr} = 0.79$, which reduces the peak heights of the fluorescence signal (see section 3.1.1), the size of the detection volume was deliberately expanded to maximize the number of detected fluorescence photons. Both effects result in a decrease of the S/B ratio.[49]

A signal with a drop of Δt is classified as fluorescence burst if a certain number of consecutive photons are below a threshold, Δt_{th} (dashed horizontal line in Figure 4A). To determine an appropriate threshold value, Δt_{th}, the original Δt trace was smoothed over n consecutive photons to reduce the signal noise. To avoid artifacts in the subsequently calculated BSD, β, the threshold value as well as the smoothing number must carefully be chosen, being aware of two problems: (1) A burst might be caused by background photons due to fluctuations in the background signal as discussed in detail in section 3.2. (2) Extensive smoothing can affect the burst size, C_t, by blurring the signal, which results in a distorted burst size distribution of the sample survey as outlined below.[60] Let us consider a close sequence of individual bursts, a large threshold value, Δt_{th}, together with a high smoothing factor, n, would lead to overlapping bursts, caused by more than one molecule transit. In contrast, a small threshold would reduce the number of selected bursts, especially because the smoothing increases the Δt values in the burst region. Thus, a small threshold might cause errors in the statistics of a burst size distribution. In addition, we point out that the theory on the density distribution of dwell times in section 3.1.2 is valid for traversing motions through the entire probe volume. Thus, one should only choose

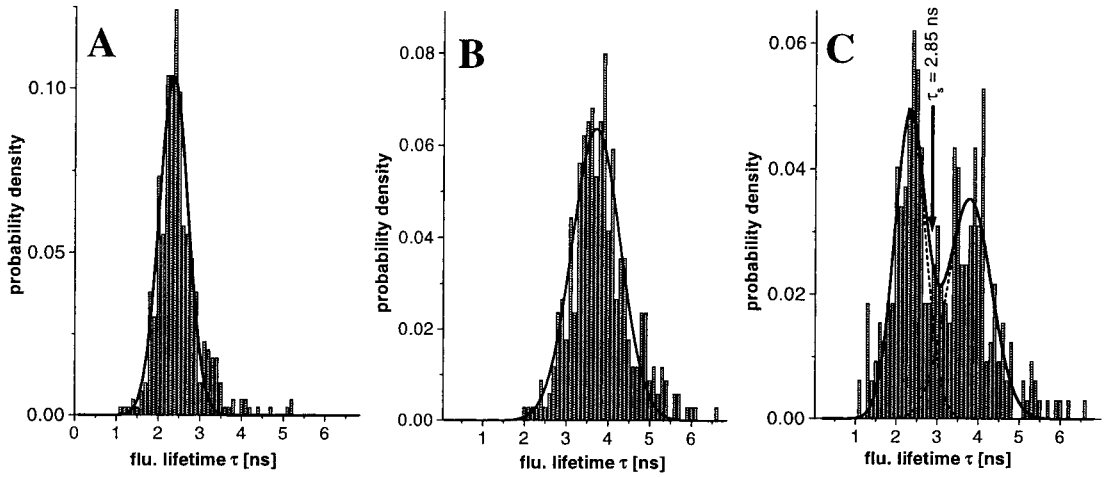

Figure 5. Fluorescence lifetime (τ) histograms: (A) 394 bursts of S(RhB), $\tau = 2.4 \pm 0.3$ ns; (B) 375 bursts of S(Rh6G), $\tau = 3.7 \pm 0.6$ ns; (C) 325 bursts of S(MIX), $\tau_1 = 2.3 \pm 0.4$ ns and $\tau_2 = 3.8 \pm 0.5$ ns. The arrow indicates the separation lifetime, $\tau_s = 2.85$ ns, to distinguish between RhB and Rh6G molecules (see text).

those parts of the burst which are caused by molecules directly traversing through the origin of the detection volume to avoid signal fractions of the burst where the molecule has left and entered the detection volume several times.[50] Therefore, we varied the threshold value as well as the smoothing factor, n, for a subsequent BSD, β, revealing the optimized value of $\Delta t_{th} = 45$ μs (log 45 = 1.65) at $n = 50$ for a stable BSD (dashed horizontal line in Figure 4A). Δt_{th} could be varied between 30 and 80 μs, without significantly changing the calculated BSD of the sample survey. Furthermore, the choice of $\Delta t_{th} = 45$ μs at a mean time lag between background photons of $\Delta t_{av} = 170$ μs ($\xi = \Delta t_{th}/\Delta t_{av} = 0.27$) results in an error probability, α, of an identification due to background photons of almost zero (eq 26; see Figure 3).

With respect to these arguments, we obtain an undisturbed burst size statistics, since we exactly select those single molecules traversing the detection volume and exclude background photons. Considering eq 20, the probability, Pm_n, that a burst is caused by a multimolecule event is smaller than 8% for $N_{av} \approx 0.08$ (see Table 1); i.e., more than 92% of all analyzed bursts are really due to single-molecule events.

Identification by Fluorescence Lifetime Distributions. For a fluorescence lifetime determination, a histogram of fluorescence arrival times, which is the second piece of information of each photon in a BIFL measurement (see Figure 1), is generated for all photons within a fluorescence burst. Subsequently, the fluorescence lifetime of every selected burst is determined, using an efficient pattern recognition technique based on a maximum likelihood estimator (MLE) (eq 31; for details see section 3.4). This is, for example, shown in the three insets (I−III) of Figure 4, giving two fluorescence bursts and some randomly selected background photons (open circles, full circles, and triangles), the response function of the laser pulse (dotted line), and the model obtained by MLE (full line). In inset I, the decay of the 221 photons, obtained from the event numbers 5007−5228 (open circles), is described by a fluorescence lifetime of $\tau = 3.9$ ns, without any scatter contribution ($\gamma = 0$), and with a $2I_r^* = 0.8$. Inset II gives the arrival times of the event numbers 9255−9350 (full circles) with $\tau = 2.0$ ns, $\gamma = 0$, and $2I_r^* = 0.6$. Inset III contains the decay of 150 background photons (full triangles), which are equivalent to the instrument response function.

All bursts, which are selected from the BIFL measurements of the three samples, S(RhB), S(Rh6G), and S(MIX), by using the same threshold criterion, are analyzed by the MLE to determine the fluorescence lifetimes, τ. The resulting histograms of the obtained fluorescence lifetime, τ, are shown in Figure 5.

The τ-histogram containing 394 analyzed bursts of S(RhB) (Figure 5A) reveals a Gaussian distribution with a mean fluorescence lifetime of $\tau_{av} = 2.4$ ns and a standard deviation of $\sigma = 0.3$ ns. The τ-histogram of the equivalent S(Rh6G) experiment with 375 selected bursts has a mean fluorescence lifetime of $\tau_{av} = 3.7 \pm 0.6$ ns. These mean values correspond closely to those obtained in precision measurements of the dyes at a higher concentration in the same solvent mixture (RhB $\tau = 2.3$ ns, Rh6G $\tau = 3.6$ ns). The standard deviations of S(RhB) and S(Rh6G) agree well with theory[58] and earlier reports.[3,44] The relative error, $\sigma/\tau = 0.15$, is equal for both dyes.

The fluorescence lifetime histogram of the approximately equimolar mixture of the two dyes, S(MIX), with 325 fluorescence bursts exhibits two overlapping Gaussian distributions peaked at $\tau_1 = 2.3 \pm 0.4$ ns and $\tau_2 = 3.8 \pm 0.5$ ns. The ratio of the areas is 1/1.03. This is concurrent to the mixing ratio of the single dye solutions used to prepare the sample (see section 2). Considering the mean lifetimes, τ_1 and τ_2, and their standard deviations in the histogram of the dye mixture (Figure 5C), the observed τ-distribution is in perfect agreement with the sum of the two distributions obtained by measurements of the single dyes (Figure 5A/B). The overlap area of the two Gaussian distributions is equivalent to 5% of the total area; i.e., 5% of all single molecule transits cannot be classified correctly.

Hence, using time-resolved SMD together with BIFL, we can identify different fluorophores with specific fluorescence lifetimes coexistently present in the same solution and reproduce a given ratio of two dyes in a dye mixture. Because the standard deviation of the fluorescence lifetime depends on the number of analyzed photons ($\sigma \propto 1/\sqrt{N}$),[55] the accuracy of this method is only sufficient for those bursts which have a certain minimum number of fluorescence photons (here 50).

Quantification by Burst Size Distributions. In view of the fact that the handling of organic compounds in dilute aqueous media is problematic due to losses caused by unspecific adsorption,[4,8] we try to investigate the question whether it is experimentally possible to describe the quantitative properties of a given sample correctly by single-molecule spectroscopy. In the following, we will demonstrate that it is even in an open volume element possible to quantify the average number of molecules in a sample, N_{av}, containing different fluorescent

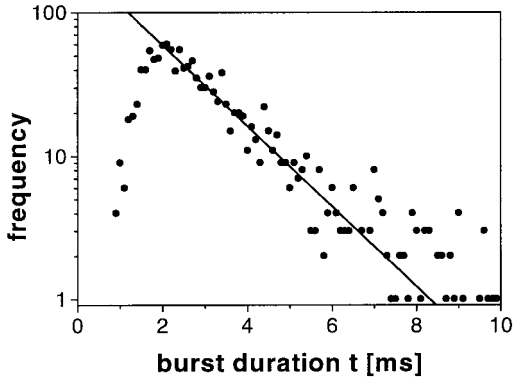

Figure 6. Burst duration distribution, $Pt_m(t)$, of all 1094 analyzed bursts and fitted curve (eq 18, straight line, fit starts at 2 ms) with a mean burst duration of $t_B = 1.55$ ms.

compounds. This is achieved by selecting bursts of a certain minimum size and by analyzing this characteristic sample survey in two steps: (1) The dye molecules are identified and sorted via their characteristic fluorescence lifetimes using the MLE. (2) Burst size distributions, β, of the sample survey allow for a subsequent quantitative analysis.

One of the parameters being necessary to describe a BSD according to eq 23 is the mean transit time, t_t, of a single molecule through the detection volume (eq 17). To determine t_t for the current experimental conditions, we analyzed the distribution of the mean burst duration for 1094 selected bursts obtained from S(RhB), S(Rh6G), and S(MIX) (Figure 6).

Taking multimolecule events into account, the data were fitted to eq 18. At an average molecule number of $N_{av} \approx 0.08$, the obtained mean burst duration, $t_B = 1.55$ ms, corresponds to a mean single-molecule transit time of $t_t(\text{BIFL}) = 1.4$ ms. In view of diffusion theory the characteristic diffusion time, $\tau_D = 0.9$ ms, obtained by FCS can also be used to evaluate the mean single molecule transit time, $t_t(\text{FCS}) = {}^4/_3\tau_D = 1.2$ ms (see section 3.1.2).[33] The agreement between the two t_t values determined by the alternative methods is satisfactory. We note that τ_D is significantly shorter than t_t, since it is a measure for peripheral and traversing transits.

In the following, we compare the different results for the average number of sample molecules, N_{av}, in the detection volume obtained by three alternative methods: (1) N_{av}(BIFL) is a fit parameter in the analysis of the BSDs using our model described in section 3.1.4 (eq 23). (2) N_{av}(FCS) is a fit parameter for the amplitude, $G(t_c = 0)$, of the autocorrelation functions using eq 28. (3) $N(\text{Exp}) = Vc(\text{Exp})$ can be calculated from the detection volume, $V = 2.65 \times 10^{-14}$ L (see section 2), and the employed dye concentration, c(Exp). c(Exp) is known from the dilution factor of the dye stock solutions at a higher concentration (5×10^{-6} M). The concentrations of the stock solutions have exactly been determined by absorption spectroscopy in ethanol, using the extinction coefficients ϵ(Rh6G, 530 nm) = 105 000 M^{-1} cm^{-1} and ϵ(RhB, 552 nm) = 107 000 M^{-1} cm^{-1}.[61]

TABLE 1: Average Number of Dye Molecules in the Open Volume Element

	solution			
	S(RhB)	S(Rh6G)	S(MIX):RhB	S(MIX):Rh6G
c_{exp} (pM)[a]	6	2	1.5	1.5
N(Exp)[a]	0.10	0.03	0.024	0.024
N_{av}(FCS)[b]	0.22 ± 0.06	0.08 ± 0.02	0.085 ± 0.041	
N_{av}(BIFL)[c]	0.29 ± 0.06	0.08 ± 0.02	0.028 ± 0.010	0.022 ± 0.010

[a] Unknown systematic errors due to dilution and adsorption. [b] Errors calculated by error propagation: uncertainty and standard deviation of the background (±10%) and signal (±4%) count rate. [c] Errors introduced by the fit procedure.

A BSD of a single-molecule experiment is obtained by plotting the number of detected fluorescence photons, C_t, within a fluorescence burst versus its frequency, $\beta(C_t)$, in the measurement. The minimum burst size is 50 photons, given by the burst threshold criterion discussed above. The BSDs and the simultaneously recorded autocorrelation curves, $G(t_c)$, of the solutions, S(RhB) (full circles) and S(Rh6G) (open circles), are shown in Figure 7A,B and Figure 7C,D, respectively.

The insets in Figure 7A,B represent two cuts in the χ^2-surface of the fit of eq 23 to the BSDs to demonstrate the well-defined minima of the variables, gI_0 and N_{av}. The analysis of the FCS data by eq 28 also takes into account the influence of the background signal to the amplitude of the autocorrelation function. The background signal was approximately $I_B \approx 6$ kHz and has been determined from the count rates of the BIFL data, which introduces an uncertainty of ±10%. This leads to a correction factor of $f_c = 5.5$ (see eq 28) for these measurement conditions. The results of the corresponding fits are summarized in Table 1.

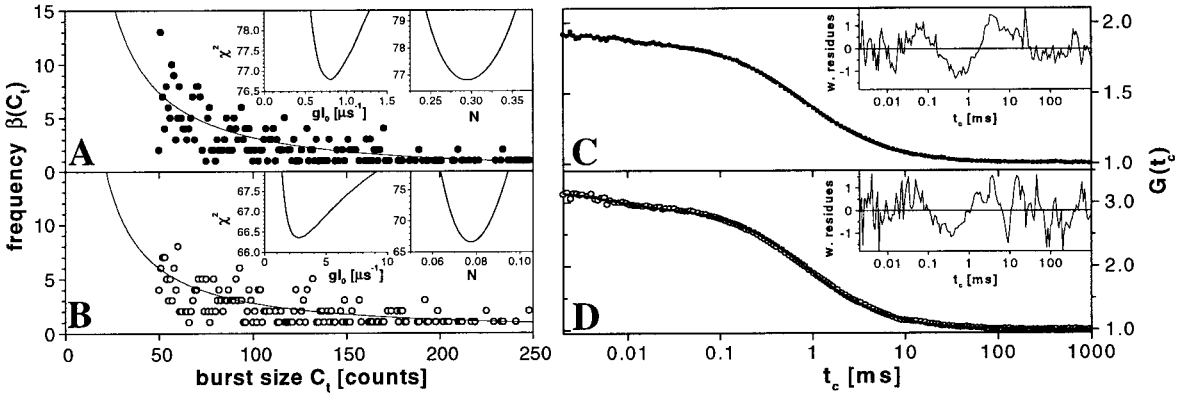

Figure 7. (A, B) Burst size distribution, $\beta(C_t,N_{av},g)$, of the single dye solutions, S(RhB) and S(Rh6G). The data are well described by eq 23 using the following parameters: (A) S(RhB) (full circles) fixed, $t_t = 1.2$ ms, $t_{mes} = 14.3$ s; fitted, $N_{av} = 0.29 \pm 0.06$, $gI_0 = (8.0 \pm 3.5) \times 10^5$ s^{-1}; (B) S(Rh6G) (open circles) fixed, $t_t = 1.2$ ms, $t_{mes} = 35.9$ s; fitted, $N_{av} = 0.08 \pm 0.02$, $gI_0 = (2.8 \pm 1.3) \times 10^6$ s^{-1}. (C, D) Fluorescence autocorrelation curves, $G(t_c)$, of the single dye solutions: recorded data (black dots) and fitted curve (eq 28) with weighted residuals (insets). The signal intensity, I_S, and the background intensity, I_B, were obtained from MCS data recorded by the correlator card: (C) S(RhB) (full circles), $I_S = (15.8 \pm 0.6)$ kHz, $I_B = (9.0 \pm 0.9)$ kHz; fitted parameters, $G(0) = 0.9$, $\tau_D = 0.89$ ms, $z_0/\omega_0 \approx 20$, $T_{1eq} = 0.08$, $t_T = 9.1$ μs; (D) S(Rh6G) (open circles), $I_S = (10.1 \pm 0.4)$ kHz, $I_B = (5.8 \pm 0.6)$ kHz; fitted parameters, $G(0) = 2.2$, $\tau_D = 0.88$ ms, $z_0/\omega_0 \approx 20$, $T_{1eq} = 0.12$, $t_T = 6.6$ μs.

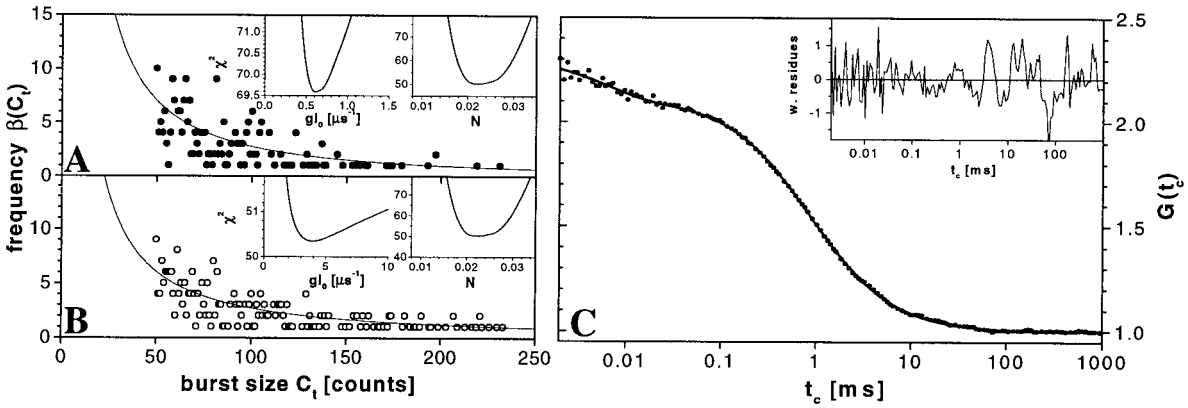

Figure 8. (A, B) Burst size distribution, $\beta(C_t,N_{av},g)$, of the mixed dye solution, S(MIX). The data are well described by eq 23 using the following parameters: fixed, $t_t = 1.2$ ms, $t_{mes} = 115.9$ s, (A) S(MIX):RhB (full circles) fitted, $N_{av} = 0.028 \pm 0.010$, $gI_0 = (6.0 \pm 3.8) \times 10^5$ s^{-1}, (B) S(MIX):Rh6G (open circles) fitted, $N_{av} = 0.022 \pm 0.010$, $gI_0 = (3.8 \pm 1.9) \times 10^6$ s^{-1}. (C) Fluorescence autocorrelation curve, $G(t_c)$, for the mixed dye solution, S(MIX): recorded data (full circles) and fitted curve (eq 28) with weighted residuals (insets), $I_S = (8.7 \pm 0.3)$ kHz, $I_B = (6.0 \pm 0.6)$ kHz; fitted parameters, $G(0) = 1.3$, $\tau_D = 0.90$ ms, $z_0/\omega_0 \approx 20$, $T_{1eq} = 0.15$, $t_T = 6.0$ μs.

The two results for the average molecule number, N_{av}(BIFL) and N_{av}(FCS), are in good agreement and describe the real concentration of the solution very well. The low values of N_{av} between 0.02 and 0.29 for the individual measurements prove that single-molecule experiments have been performed in the open volume element. The concentrations N_{av}(BIFL) and N_{av}(FCS) only differ by a factor 2−3 from N(Exp). This difference may be explained by minor dilution errors (the dilution factor was 1:10[8]), adsorption effects, and impurities in the solvent mixture, which cannot be totally avoided.

The maximum experimental detection rate, gI_0, which is the product of the experimental detection factor, g, and the irradiance, I_0, and its standard deviation are also obtained by the fits of eq 23 to the BSDs of S(RhB) and S(Rh6G): gI_0(S(RhB)) $= (8.0 \pm 3.5) \times 10^5$ s^{-1} and gI_0(S(Rh6G)) $= (2.8 \pm 1.3) \times 10^6$ s^{-1}. By comparison of the two values of gI_0 for S(RhB) and S(Rh6G), a ratio of the experimental detection factors, R_g(BIFL) $= g_{S(Rh6G)}/g_{S(RhB)} = 3.5 \pm 1.8$, is obtained. The detection efficiency ratio can also be measured by comparing the fluorescence emission spectra of two equimolar solutions (10^{-7} M) of Rh6G and RhB under the same conditions as used in the single-molecule experiment (solvent mixture, excitation wavelength $\lambda = 522$ nm). Regarding the transmission characteristics of the emission filter (HQ 582/50), we evaluate a ratio of the experimental detection factors, R_g(Spectra) $= g_{Rh6G}/g_{RhB} = 3.0$. These consistent results for R_g give further confidence to our BSD theory. In view of eq 6 or 16, we note that the difference between the experimental detection factors, g_{Rh6G} and g_{RhB}, has two dye specific reasons: Rh6G has a higher absorption cross section, σ_{01}, at 522 nm as well as a higher fluorescence quantum efficiency, Φ_F, and consequently a longer fluorescence lifetime, τ (see Figure 5), than Rhodamine B.[62]

To determine the concentration of each dye compound in the mixed solution, S(MIX), it is necessary to classify the bursts by separating the distribution in Figure 5C in two classes: Rhodamine 6G molecules (S(MIX):Rh6G) and Rhodamine B molecules (S(MIX):RhB). Because we distinguish between the two kinds of molecules via their characteristic fluorescence lifetime, τ, we must define a separation fluorescence lifetime, τ_s, where the classification probability for the characteristic fluorescence lifetimes, τ(RhB) $= 2.3$ ns and τ(Rh6G) $= 3.6$ ns, is equal. In other words, we have to find the lifetime, τ_s, characteristic for a certain decay which is equally well described by τ(RhB) or τ(Rh6G), defined by equal values of $2I_r^*$ in eq 31. τ_s slightly depends on the burst size, C_t. Using our experimental parameters in eqs 30 and 31, the τ_s values range between 2.9 and 2.8 ns for $C_t \leq 108$ photons and are smaller than 2.8 ns for $C_t > 108$ photons. Because most of the analyzed fluorescence bursts have less than 108 photons, we assigned a burst to a certain dye class using a separation fluorescence lifetime of $\tau_s = 2.85$ ns (vertical arrow in Figure 5C): S(MIX): RhB $\tau \leq 2.8$ ns and S(MIX):Rh6G $\tau > 2.8$ ns.

It is important to note that this separation would also work for mixtures of different dye molecules with excess of one kind. Because the fluorescence lifetime is a dye-specific property, only the widths (i.e., the standard deviation, σ) and the overlap of the different lifetime distributions but not the ratio of the different dye concentrations determine the statistical accuracy of an identification of a single dye molecule via its fluorescence lifetime, τ.

From this classification we obtain separate burst size histograms, $\beta(C_t)$, for each dye of S(MIX) using the procedure described above. They are shown in Figure 8A (full circles) for S(MIX):RhB and in Figure 8B (open circles) for S(MIX): Rh6G. A fit (Figure 8A/B, solid line) of eq 23 to these data results in values of N_{av}(BIFL) $= 0.028 \pm 0.010$ and $gI_0 = (6.0 \pm 3.8) \times 10^5$ s^{-1} for S(MIX):RhB and of N_{av}(BIFL) $= 0.022 \pm 0.010$ and $gI_0 = (3.8 \pm 1.9) \times 10^6$ s^{-1} for S(MIX):Rh6G (see Table 1). The obtained results for the dye specific detection rates, gI_0, are in good agreement with the data obtained in the single dye mixture.

For each dye, the value of N_{av}(BIFL) ≈ 0.025 corresponds very well with the employed concentration, N(Exp) $= 0.024$, revealing the intended equimolar mixture. The simultaneously recorded FCS curve (full circles, Figure 8C) cannot distinguish between the two fluorophores because of the same diffusion coefficient of both dyes. Thus, a fit of eq 28 to this correlation curve (solid line, Figure 8C) results in an overall average number of dye molecules in V of N_{av}(FCS) $= 0.085 \pm 0.041$. (The large uncertainty in N_{av}(FCS) is introduced by the standard deviation of the background, I_B, and signal count rate, I_S, and calculated by error propagation.) The value of N_{av}(FCS) is close to the sum of the values determined from the burst size distributions using BIFL, N_{av}(BIFL, RhB + Rh6G) $= 0.022 + 0.028 = 0.050 \pm 0.010$.

Additionally, this method opens up an elegant way to determine the detection efficiency, Ψ, of the optical setup, since the expression $g = \Psi\Psi_{electr}\Phi_F\sigma_{01}(\lambda_{ex})\gamma$ (eq 16) contains experimentally known parameters: the fluorescence quantum yields, $\Phi_F \approx 0.90$ for Rh6G and $\Phi_F \approx 0.58$ for RhB (assuming

$\Phi_F = 1$ for $\tau = 4$ ns), the absorption cross sections, $\sigma_{01}(522\ \text{nm}) = 3.1 \times 10^{-16}$ cm^2 for Rh6G and $\sigma_{01}(522\ \text{nm}) = 1.3 \times 10^{-16}$ cm^2 for RhB, $\gamma = 2.6 \times 10^{18}$ J^{-1} for $\lambda = 522$ nm, and the detection efficiency of the detection electronics, $\Psi_{electr} = 0.79$ (see section 3.1.1). At a focal excitation irradiance of $I_0 = 1.5 \times 10^5$ W/cm^2 (see section 2), the values of $gI_0 = (2.8 \pm 1.3) \times 10^6$ s^{-1} for Rh6G and $gI_0 = (8 \pm 3.5) \times 10^5$ s^{-1} for RhB result in values of the detection efficiency of $\Psi_{Rh6G} = (3.3 \pm 1.5)\%$ and $\Psi_{RhB} = (3.5 \pm 1.5)\%$. These nearly identical detection efficiencies reveal the minor dye specific difference in the transmission characteristics of the emission filter with respect to the total fluorescence emission spectrum (HQ 582/50: S(Rh6G) 53%, S(RhB) 65%). Furthermore, the values of Ψ are in agreement with estimated values based on theoretical calculations, which have been reported previously for similar setups.[63,64]

5. Conclusion

The procedure of identifying single molecules by time-resolved fluorescence spectroscopy using our recently developed BIFL method is capable to distinguish between different kinds of dyes and reproduces a given ratio of fluorescent molecules in a mixture. Furthermore, BIFL allows one to establish an exact burst size distribution for a sample survey. Using the theoretical described formalism for BSD, it is possible to determine the concentration of dyes by measurements in an open volume element. The results obtained by this method are consistent with results from FCS measurements. In contrast to FCS, this method analyzes each single event separately, and thus, it should be able to detect even extreme small fractions of fluorescent molecules in excesses of dye molecules with other fluorescence properties. Additionally, our method opens up a simple way to determine the detection efficiency of an experimental single-molecule setup. The ease of confocal detection and very simple sample handling make BIFL an ideal candidate for various applications in ultrasensitive analytical chemistry, biochemistry, and pharmacology using fluorescent dyes.

Acknowledgment. We are grateful to J. Troe, K. H. Drexhage, and J. Wolfrum for support of this work. We thank J. Enderlein and J. Stephan for many valuable discussions and for reading parts of the manuscript. This work was supported by the Bundesministerium für Bildung, Wissenschaft, Forschung und Technologie, Grant 0310806.

References and Notes

(1) Soper, S. A.; Davis, L. M.; Brooks Shera, E. *J. Opt. Soc. Am. B* **1992**, *9*, 1761−1769.

(2) Zander, C.; Sauer, M.; Drexhage, K. H.; Ko, D.-S.; Schulz, A.; Wolfrum, J.; Brand, L.; Eggeling, C.; Seidel, C. A. M. *Appl. Phys. B* **1996**, *63*, 517−523.

(3) Müller, R.; Zander, C.; Sauer, M.; Deimel, M.; Ko, D.-S.; Siebert, S.; Arden-Jacob, J.; Deltau, G.; Marx, N. J.; Drexhage, K. H.; Wolfrum, J. *Chem. Phys. Lett.* **1996**, *262*, 716−722.

(4) Enderlein, J.; Goodwin, P. M.; van Orden, A.; Ambrose, W. P.; Erdmann, R.; Keller, R. A. *Chem. Phys. Lett.* **1997**, *270*, 464−470.

(5) Sauer, M.; Arden-Jacob, J.; Drexhage, K.-H.; Göbel, F.; Lieberwirth, U.; Mühlegger, K.; Müller, R.; Wolfrum, J.; Zander, C. *Bioimaging* **1998**, *6*, 14−24.

(6) Chen, D.; Dovichi, N. J. *Anal. Chem.* **1996**, *68*, 690−696.

(7) Ambrose, W. P.; Goodwin, P. M.; Jett, J. H.; Johnson, M. E.; Martin, J. C.; Marrone, B. L.; Schecker, J. A.; Wilkerson, C. W.; Keller, R. A.; Haces, A.; Shih, P.-J.; Harding, J. D. *Ber. Bunsen-Ges. Phys. Chem.* **1993**, *97*, 1535−1542.

(8) Dörre, K.; Brakmann, S.; Brinkmeier, M.; Han, K.-T.; Riebeseel, K.; Schwille, P.; Stephan, J.; Wetzel, T.; Lapczyna, M.; Stuke, M.; Bader, R.; Hinz, M.; Seliger, H.; Holm, J.; Eigen, M.; Rigler, R. *Bioimaging* **1997**, *5*, 139−152.

(9) Eggeling, C.; Fries, J. R.; Brand, L.; Günther, R.; Seidel, C. A. M. *Proc. Natl. Acad. Sci. U.S.A.* **1998**, *95*, 1556−1561.

(10) Affleck, R. L.; Ambrose, W. P.; Demas, J. N.; Goodwin, P. M.; Schecker, J. A.; Wu, M.; Keller, R. A. *Anal. Chem.* **1996**, *68*, 2270−2276.

(11) Mets, Ü.; Rigler, R. *J. Fluoresc.* **1994**, *4*, 259−264.

(12) Keller, R. A.; Ambrose, W. P.; Goodwin, P. M.; Jett, J. H.; Martin, J. C.; Wu, M. *Appl. Spectrosc.* **1996**, *50*, 12A−32A.

(13) Mertz, J.; Xu, C.; Webb, W. W. *Opt. Lett.* **1995**, *20*, 2532−2534.

(14) Brand, L.; Eggeling, C.; Zander, C.; Drexhage, K. H.; Seidel, C. A. M. *J. Phys. Chem.* **1997**, *101*, 4313−4321.

(15) Eggeling, C.; Brand, L.; Seidel, C. A. M. *Bioimaging* **1997**, *5*, 105−115.

(16) Sauer, M.; Zander, C.; Müller, R.; Ullrich, B.; Drexhage, K. H.; Kaul, S.; Wolfrum, J. *Appl. Phys. B* **1997**, *65*, 427−431.

(17) Lyon, W. A.; Nie, S. *Anal. Chem.* **1997**, *69*, 3400−3405.

(18) Zander, C.; Drexhage, K. H. *J. Fluoresc.* **1996**, *7*, 37S−39S.

(19) Zander, C.; Drexhage, K.-H.; Han, K.-T.; Wolfrum, J.; Sauer, M. *Chem. Phys. Lett.* **1998**, in press.

(20) Goodwin, P. M.; Ambrose, W. P.; Keller, R. A. *Acc. Chem. Res.* **1996**, *29*, 607−613.

(21) Li, L.-Q.; Davis, L. M. *Appl. Opt.* **1995**, *34*, 3208−3217.

(22) Lermer, N.; Barnes, M. D.; Kung, C.-Y.; Whitten, W. B.; Ramsey, J. M. *Anal. Chem.* **1997**, *69*, 2115−2121.

(23) Nie, S.; Chiu, D. T.; Zare, R. N. *Anal. Chem.* **1995**, *67*, 2849−2857.

(24) Rigler, R.; Widengren, J. In *BioScience*; Klinge, B., Owman, C., Eds.; Lund University Press: Lund, Sweden, 1990; pp 180−183.

(25) Dickson, R. M.; Cubitt, A. B.; Tsien, R. Y.; Moerner, W. E. *Nature* **1997**, *388*, 355−358.

(26) Dickson, R. M.; Norris, D. J.; Tzeng, Y. L.; Moerner, W. E. *Science* **1996**, *274*, 966−969.

(27) Xu, X.-H.; Yeung, E. S. *Science* **1997**, *275*, 1106−1109.

(28) Rigler, R.; Mets, Ü.; Widengren, J.; Kask, P. *Eur. Biophys. J.* **1993**, *22*, 169−175.

(29) Qian, H.; Elson, E. L. *Appl. Opt.* **1991**, *30*, 1185−1195.

(30) Enderlein, J.; Robbins, D. L.; Ambrose, W. P.; Goodwin, P. M.; Keller, R. A. *J. Phys. Chem. B* **1997**, *101*, 3626−3632.

(31) Whitten, W. B.; Ramsey, J. M. *Appl. Spectrosc.* **1992**, *46*, 1587−1589.

(32) Rigler, R.; Mets, Ü. *SPIE* **1992**, *1921*, 239−248.

(33) Eigen, M.; Rigler, R. *Proc. Natl. Acad. Sci. U.S.A.* **1994**, *91*, 5740−5747.

(34) Rigler, R. *J. Biotech.* **1995**, *41*, 177−186.

(35) Schwille, P.; Meyer-Almes, F. J.; Rigler, R. *Biophys. J.* **1997**, *72*, 1878−1886.

(36) Wiener, N. *Extrapolation, Interpolation, and Smoothing of Stationary Time Series*; MIT Press: Cambridge, MA, 1949.

(37) Magde, D.; Elson, E. L.; Webb, W. W. *Phys. Rev. Lett.* **1972**, *29*, 705−708.

(38) Elson, E. L.; Magde, D. *Biopolymers* **1974**, *13*, 1−27.

(39) Ehrenberg, M.; Rigler, R. *Chem. Phys.* **1974**, *4*, 390−401.

(40) Thompson, N. L. In *Topics in Fluorescence Spectroscopy, Volume 1: Techniques*; Lakowicz, J. R., Ed.; Plenum Press: New York, 1991; pp 337−378.

(41) Koppel, D. E. *Phys. Rev. A* **1974**, *10*, 1938−1945.

(42) Enderlein, J.; Köllner, M. *Bioimaging* **1998**, *6*, 3−13.

(43) Tellinghuisen, J.; Goodwin, P. M.; Ambrose, W. P.; Martin, J. C.; Keller, R. A. *Anal. Chem.* **1994**, *66*, 64−72.

(44) Zander, C.; Sauer, M.; Drexhage, K. H.; Ko, D. S.; Schulz, A.; Wolfrum, J.; Brand, L.; Eggeling, C.; Seidel, C. A. M. *Appl. Phys. B* **1996**, *63*, 517−523.

(45) Widengren, J.; Mets, Ü.; Rigler, R. *J. Phys. Chem.* **1995**, *99*, 13368−13379.

(46) Qian, H. *Biophys. Chem.* **1990**, *38*, 49−57.

(47) Enderlein, J.; Robbins, D. L.; Ambrose, W. P.; Keller, R. A. *J. Phys. Chem. B*, submitted for publication.

(48) Saleh, B. *Photonelectron Statistics*; Springer-Verlag: Berlin, 1977.

(49) Eggeling, C.; Widengren, J.; Rigler, R.; Seidel, C. A. M. *Anal. Chem.* **1998**, *70*, 2651−2659.

(50) Ko, D.-S.; Sauer, M.; Nord, S.; Müller, R.; Wolfrum, J. *Chem. Phys. Lett.* **1997**, *269*, 54−58.

(51) Edman, L.; Mets, Ü.; Rigler, R. *Proc. Natl. Acad. Sci. U.S.A.* **1996**, *93*, 6710−6715.

(52) Aragón, S. R.; Pecora, R. *J. Chem. Phys.* **1976**, *64*, 1791−1803.

(53) Kask, P.; Günther, R.; Axhausen, P. *Eur. Biophys. J.* **1997**, *25*, 163−169.

(54) Kotze, T. J.v. W.; Gokhale, D. V. *J. Stat. Comput. Simul.* **1980**, *12*, 1−13.

(55) Hall, P.; Selinger, B. *J. Phys. Chem.* **1981**, *85*, 2941−2946.

(56) Köllner, M.; Fischer, A.; Arden-Jacob, J.; Drexhage, K. H.; Müller, R.; Seeger, S.; Wolfrum, J. *Chem. Phys. Lett.* **1996**, *250*, 355−360.

(57) Köllner, M.; Wolfrum, J. *Chem. Phys. Lett.* **1992**, *200*, 199−204.
(58) Köllner, M. *Appl. Opt.* **1993**, *32*, 806−820.
(59) Kullback, S. *Information Theory and Statistics*; John Wiley & Sons: New York, 1959.
(60) Enderlein, J.; Robbins, D. L.; Ambrose, W. P.; Goodwin, P. M.; Keller, R. A. *Bioimaging* **1997**, *5*, 88−98.
(61) Brackmann, U. *Lambdachrome Laser Dyes*; Lambda Physik GmbH: Göttingen, Germany, 1994.
(62) Vogel, M.; Rettig, W.; Sens, R.; Drexhage, K. H. *Chem. Phys. Lett.* **1988**, *147*, 452−460.
(63) Shera, E. B.; Seitzinger, N. K.; Davis, L. M.; Keller, R. A.; Soper, S. A. *Chem. Phys. Lett.* **1990**, *174*, 553−557.
(64) Nie, S.; Chiu, D. T.; Zare, R. N. *Science* **1994**, *266*, 1018−1021.